13th U.S. National Combustion Meeting
Organized by the Central States Section of the Combustion Institute
March 19–22, 2023
College Station, Texas

Characterization of Nascent Soot Particles from Acetylene Pyrolysis: A Molecular Modeling Perspective

Khaled Mosharraf Mukut[1], Anindya Ganguly[2], Eirini Goudeli[2], Georgios Kelesidis[3], and Somesh Roy[1,*]

[1]*Department of Mechanical Engineering, Marquette University, Milwaukee, WI 53233, U.S.A*
[2]*Department of Chemical Engineering, University of Melbourne, Victoria, Australia*
[3] *Department of Mechanical and Process Engineering, ETH Zürich, Sonneggstrasse 3, CH-8092 Zürich, Switzerland*
[*]*Corresponding author:* `somesh.roy@marquette.edu`

Abstract: Soot or black carbons are combustion-generated carbonaceous nanoparticles formed during the incomplete combustion of hydrocarbon fuels. The complexity of hydrocarbon systems often makes it difficult to investigate the fundamentals of soot formation experimentally. To address this, this study uses reactive molecular dynamics simulations with reactive force field (ReaxFF) potentials. The current work focuses on the formation and evolution of soot during acetylene pyrolysis. The analysis provides insights into the physicochemical aspects of soot formation and the maturation of incipient soot particles. In this work, we focus on the evolution and interdependence of features such as the number of carbon atoms, number of aromatic rings, mass, C/H ratio, the radius of gyration, atomic fractal dimension, surface area, volume, and density. Based on the physicochemical features, two distinct classes of nascent soot can be observed. These are termed type-1 and type-2 particles. The type-1 particles show significant morphological evolution, while the type-2 particles show chemical restructuring without significantly changing the morphology. Qualitative correlations of various degrees are also observed between some of these morphological features.
Keywords: Morphology, Soot, ReaxFF, Molecular Dynamics, Physicochemical Properties

1. Introduction

Soot, also known as black carbon, is a byproduct of incomplete combustion of hydrocarbon fuels [1] that can cause serious health issues such as lung cancer [2] and cardiovascular disease [3]. It also contributes to global warming and the melting of Arctic ice [4]. Understanding the formation and evolution of soot is crucial to regulating and controlling its negative effects.

The evolution of solid soot particulates from gaseous species is a complex process that is not fully understood. It is believed to occur through a series of complex physicochemical events including the formation of gas phase soot precursor molecules such as polycyclic aromatic hydrocarbons (PAHs), nucleation of nascent soot particles, surface growth, formation of aggregates, and fragmentation and oxidation of soot particles. Each of these steps plays a role in the formation and evolution of soot particles.

The formation of soot particles, specifically the nucleation process, is not well understood. Researchers believe it starts with small gas-phase precursor molecules, such as acetylene, which lead

to the formation of solid or solid-like primary particles containing PAHs like benzene, pyrene and coronene [5–7]. These primary particles then grow due to surface interactions and coalescence to form larger soot particles. However, the exact chemical pathways are unknown and numerical models of soot formation rely on empirical approximations. These approximations include assumptions about particle shape [8, 9], density [10], and chemical reactions [8, 11].

Reactive molecular dynamics (RMD) simulation is becoming a popular tool for studying the difficult physicochemical changes that occur during soot nucleation [12–15]. The ReaxFF potential [16], a reactive force field developed for carbon, hydrogen, and oxygen chemistry (CHO-parameters [17, 18]), is commonly used in RMD simulations of soot-relevant systems. This potential can capture the evolution of hydrocarbon systems at a range of temperatures and pressures and is based on bond order between atoms, which carries valuable information about bond breakage and formation. RMD simulations can provide detailed structural information at the atomic scale, making it a useful tool for analyzing nascent soot particles and extracting critical morphological information and correlations.

The present study aims to use reactive molecular dynamics (RMD) simulations to mimic the pyrolysis of acetylene at different temperatures. By doing this, the study aims to generate many nascent soot particles at various stages of development, and then to analyze the physical and chemical properties of these particles to gain a better understanding of how they evolve.

2. Numerical Methods

The present study conducts a series of RMD simulations to investigate the formation of primary soot particles from acetylene pyrolysis. The simulations were run at four different temperatures (1350K, 1500K, 1650K, and 1800K) to capture soot particles from various thermally activated systems. The RMD simulations were run using the Large-scale Atomic/Molecular Massively Parallel Simulator (LAMMPS) [19] software. The ReaxFF potential for hydrocarbons [16, 20] was used to capture the chemical changes (bond breakage and formation) during the molecular collisions between the acetylene molecules. The coordinates of each atom were calculated and updated using the velocity-Verlet algorithm [21] in conjunction with the Nose-Hoover thermostat [22] with a T_{damp} value of 10 fs. A constant number, volume, and temperature (NVT) ensemble strategy was used to run each simulation up to 10 ns. The simulation results were probed every 0.10 ns, and the meaningful clusters of hydrocarbons that resemble primary soot particles were isolated, cataloged, and analyzed. Features such as surface area and volume of primary particles were calculated using MSMS software developed by Sanner [23] and other physicochemical characteristics were analyzed mostly using MAFIA-MD [24]. The open visualization tool (OVITO) [25] was used for visualization of the molecular clusters.

The primary focus of this study is to shed light on the chemical and morphological features of incipient soot particles obtained from RMD simulations. To achieve this, a set of physical, morphological and chemical attributes are calculated for each particle, and machine learning techniques such as k-means clustering [26] and t-distributed stochastic neighbor embedding (t-SNE) [27] are used to classify the soot particles based on these attributes. Additionally, statistical and physical correlated-ness between the physicochemical properties are explored using Kendall's Tau [28] correlation to gain deeper insights into the soot formation process.
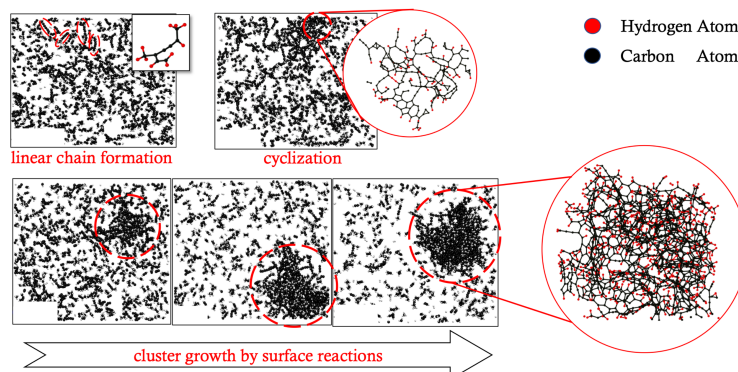
3. Results and Discussion

Figure 1: Formation and evolution of incipient soot cluster during acetylene pyrolysis at 1650 K

The present study conducts a series of reactive molecular dynamics (RMD) simulations of one thousand acetylene molecules in a semi-infinite domain at four different temperatures. The system of atoms goes through various chemical and physical interactions, leading to the formation of larger atomic clusters through the pyrolysis of acetylene. The process starts with the acetylene molecules combining to form small linear chains, then transforming into cyclic structures. After cyclization, the small clusters grow due to bond formation at the surface and internal reorganization, resulting in larger atomic clusters that resemble nascent soot particles. The evolution of one of these atomic clusters is illustrated in Figure 1, where carbon and hydrogen atoms are represented by black and red dots respectively. Similar formation mechanisms have also been reported by contemporary literatures [29, 30] in carbon-black simulations.

The nascent soot clusters obtained from the RMD simulations are tracked and extracted at different timesteps in order to capture their growth. From these simulations, 3324 nascent soot clusters were extracted at various stages of evolution. These clusters range from 102 atoms to 2303 atoms. Using two unsupervised machine learning techniques, k-means clustering [26] and t-dispersion stochastic neighbor embedding (t-SNE) [27], the particles were classified into two classes based on their physicochemical properties. These two classes are referred to as "type-1" and "type-2" particles. The resulting t-SNE diagram showed that similar particles fall into a nearly continuous size range. For example, the type-1 particles have a lower total number of atoms (102-1099) whereas type-2 particles have a higher number of total atoms (1034-2303). In total, the study obtained 670 type-1 and 2654 type-2 nascent particles from a total 3324 particles.

In this work, we investigate some physicochemical features of soot particles, including mass, number of atoms, C/H ratio, atomic fractal dimension (as defined in [30]), volume, surface area, density, particle radius, and presence of cyclic structures.

The internal C/H ratio of nascent soot particles changes as they grow and evolve. To analyze this change, particles are divided into spherical strips and the C/H ratio in each strip is measured, called the local C/H ratio. The ratio of local C/H ratio and the overall particle C/H ratio (termed as the global C/H ratio) is plotted against the normalized radial distance from the center of mass (by radius of gyration R_g). In Fig. 2, type-1 particles (bottom) have a slow increase in local C/H ratio,

3

while type-2 particles (top) have a rapid increase in local C/H ratio, reaching a peak value 1.7 times the global C/H ratio. This suggests that type-2 particles have a denser central region spanning a larger area than type-1 particles.
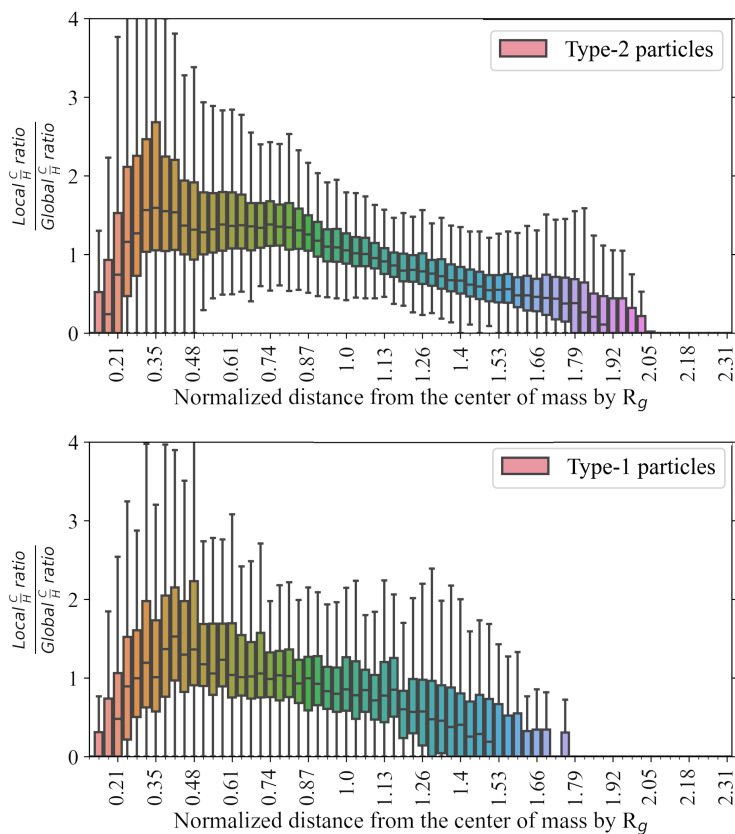

Figure 2: Radial distribution of C/H ratio in nascent particles as a function of normalized radial distance from the center of mass.

Surface area and volume are important metrics used in contemporary soot models. Fig. 3 presents the evolution of particle volume and surface area for both type-1 and type-2 particles as a function of the number of atoms in the particles. The correlation between the particle volume and number of atoms is shown in Fig. 3(a) and it indicates an excellent correlation for both type-1 and type-2 particles. The correlation coefficient is very close to unity for type-1 particles, indicating a strong correlation, and still very close to unity for type-2 particles. The relationship between particle volume and number of atoms remains consistent across all simulation temperatures, indicating that the relationship is not affected by temperature.

Figure 3(b) compares surface area for type-1 and type-2 particles. A strong correlation is observed between surface area and total number of atoms for type-1 particles, but not for type-2 particles. This is due to a transition from initial linear growth to extensive surface reorganization as particles transition from type-1 to type-2, caused by the graphitization of the surface. Temperature can accelerate this process, with higher temperatures resulting in faster growth of larger particles. Similar conclusions can be drawn for other morphological features as well.

Figure 4 illustrates the relationship between particle volume, surface area, number of ring structures and particle mass. The correlation coefficients (τ) are reported separately for both types. The
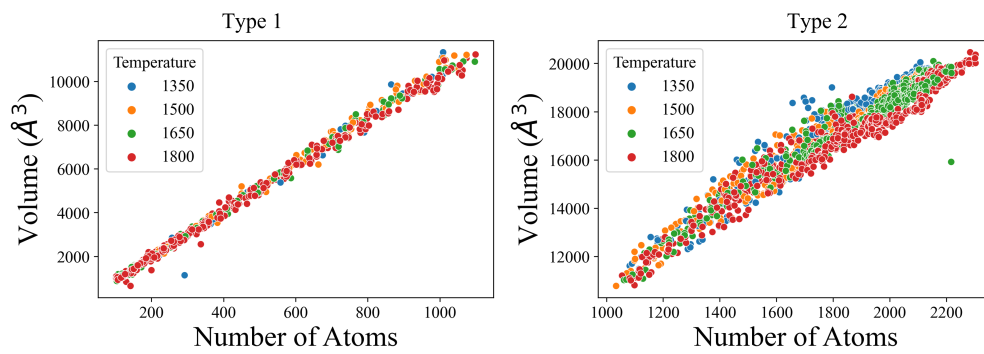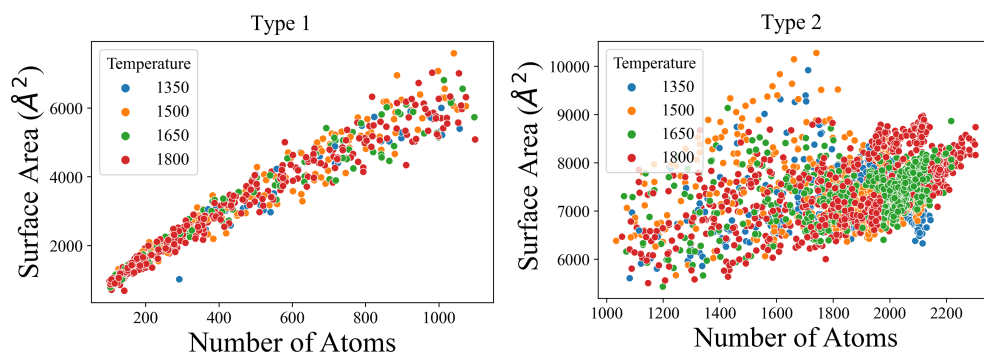
(a) Particle volume

(b) Surface area

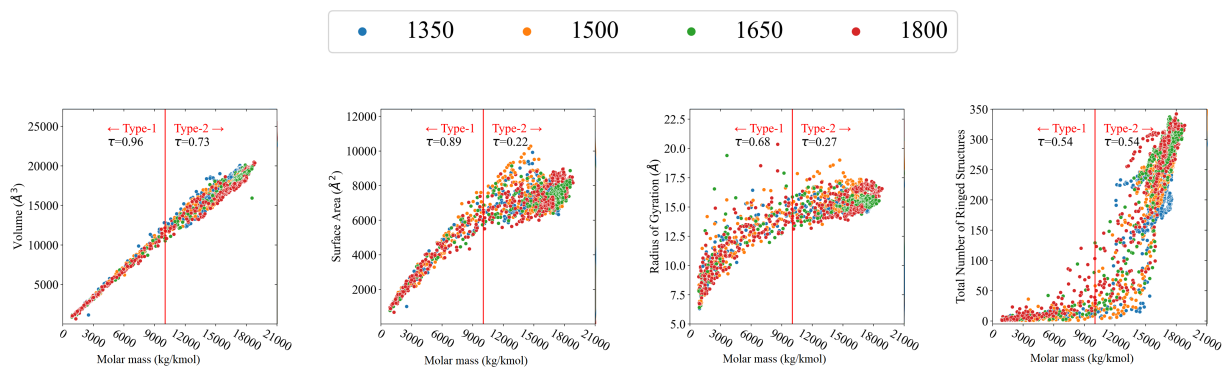Figure 3: Variation of particle volume and surface area at different temperatures.

Figure 4: Variation in physicochemical features with radius of gyration

transition between types occurs at around 10050 kg/kmol, with type-1 particles to the left of the line and type-2 particles to the right.

Fig. 4 shows the correlation between the mass of particles (type-1 and type-2) and their properties such as volume, surface area, and radius of gyration. It is observed that there is a linear correlation between volume and surface area, and a nonlinear correlation between the radius of gyration and mass. However, the correlation between the total number of ring structures and mass is not as strong. The correlation remains unchanged with temperature, but there is a sharp increase in the total number of ring structures as the particles transition from type-1 to type-2. These correlations suggest that, for type-1 particles, morphological evolution plays the dominant role in the growth of particles, while for type-2 particles, chemical evolution plays a more important role.

Looking at other physicochemical features, it is found that the variation in characteristics such as density, radius of gyration, surface area, and volume is much less pronounced in type-2 particles than in type-1. This is because as particles shift from type-1 to type-2, the process of evolution changes from morphological and physical to chemical. As a result, the atomic fractal dimension (as defined in [30]) increases from 2.1 to 2.5, creating more spherical particles. The particle C/H ratio decreases from 2.7 to 2.3 as more rings are formed. Between type-1 and type-2 particles, the density does not vary much and stays close to 1.51 g/cm^3. It is also notable that among the ring structures found in the soot cluster, the fraction of 6-membered rings greatly increases after the transition from type-1 to type-2, while the fractions of 5- and 7-membered rings decrease as they reorganize into the more stable 6 membered structures.

4. Conclusions

The study found that nascent soot particles contain both ring and non-ring structures, and that the morphological features of these particles are often correlated with each other and with the particle size. However, the strength and nature of this correlation varies between different types of particles. Type-1 particles tend to have a stronger correlation between morphological features and size than type-2 particles. Overall, type-1 particles were found to have a more prominent morphological evolution and orderedness than type-2 particles, while type-2 particles were found to have a more prominent and ordered chemical evolution. Additionally, type-2 particles have less variation in morphological features than type-1 particles.

5. Acknowledgements

References

[1] H. A. Michelsen, M. B. Colket, P.-E. Bengtsson, A. D'Anna, P. Desgroux, B. S. Haynes, J. H. Miller, G. J. Nathan, H. Pitsch, and H. Wang, A Review of Terminology Used to Describe Soot Formation and Evolution under Combustion and Pyrolytic Conditions, ACS Nano 14 (2020) 12470–12490. DOI: 10.1021/acsnano.0c06226.

[2]   N. R. Jacobsen, G. Pojana, P. White, P. Møller, C. A. Cohn, K. S. Korsholm, U. Vogel, A. Marcomini, S. Loft, and H. Wallin, Genotoxicity, cytotoxicity, and reactive oxygen species induced by single-walled carbon nanotubes and C60 fullerenes in the FE1-Muta^{TM}Mouse lung epithelial cells, Environ. Mol. Mutagen. 49 (2008) 476–487. DOI: 10.1002/em.20406.

[3]   M. Jerrett, R. T. Burnett, B. S. Beckerman, M. C. Turner, D. Krewski, G. Thurston, R. V. Martin, A. van Donkelaar, E. Hughes, Y. Shi, S. M. Gapstur, M. J. Thun, and C. A. P. Iii, Spatial Analysis of Air Pollution and Mortality in California, Am. J. Respir. Crit. Care Med. (2013), URL: https://www.atsjournals.org/doi/10.1164/rccm.201303-0609OC.

[4]   J. Hansen and L. Nazarenko, Soot climate forcing via snow and ice albedos, Proc. Natl. Acad. Sci. U.S.A. 101 (2004) 423–428. DOI: 10.1073/pnas.2237157100.

[5]   R. A. Dobbins and H. Subramaniasivam, Soot Precursor Particles in Flames, in: Soot Formation in Combustion, Springer, Berlin, Germany, 1994, pp. 290–301, DOI: 10.1007/978-3-642-85167-4_16.

[6]   M. Balthasar and M. Kraft, A stochastic approach to calculate the particle size distribution function of soot particles in laminar premixed flames, Combust. Flame 133 (2003) 289–298. DOI: 10.1016/S0010-2180(03)00003-8.

[7]   B. Wang, S. Mosbach, S. Schmutzhard, S. Shuai, Y. Huang, and M. Kraft, Modelling soot formation from wall films in a gasoline direct injection engine using a detailed population balance model, Appl. Energy 163 (2016) 154–166. DOI: 10.1016/j.apenergy.2015.11.011.

[8]   M. Frenklach, Reaction mechanism of soot formation in flames, Phys. Chem. Chem. Phys. 4 (2002) 2028–2037. DOI: 10.1039/B110045A.

[9]   K. M. Leung, R. P. Lindstedt, and W. P. Jones, A simplified reaction mechanism for soot formation in nonpremixed flames, Combust. Flame 87 (1991) 289–305. DOI: 10.1016/0010-2180(91)90114-Q.

[10]   S. Mosbach, M. S. Celnik, A. Raj, M. Kraft, H. R. Zhang, S. Kubo, and K.-O. Kim, Towards a detailed soot model for internal combustion engines, Combust. Flame 156 (2009) 1156–1165. DOI: 10.1016/j.combustflame.2009.01.003.

[11]   S. P. Roy, P. G. Arias, V. R. Lecoustre, D. C. Haworth, H. G. Im, and. Trouvé, Development of High Fidelity Soot Aerosol Dynamics Models using Method of Moments with Interpolative Closure, Aerosol Sci. Technol. 48 (2014) 379–391. DOI: 10.1080/02786826.2013.878017.

[12]   C. A. Schuetz and M. Frenklach, Nucleation of soot: Molecular dynamics simulations of pyrene dimerization, Proc. Combust. Inst. 29 (2002) 2307–2314. DOI: 10.1016/S1540-7489(02)80281-4.

[13]   Q. Mao, A. C. T. van Duin, and K. H. Luo, Formation of incipient soot particles from polycyclic aromatic hydrocarbons: A ReaxFF molecular dynamics study, Carbon 121 (2017) 380–388. DOI: 10.1016/j.carbon.2017.06.009.

[14]   S. Han, X. Li, F. Nie, M. Zheng, X. Liu, and L. Guo, Revealing the Initial Chemistry of Soot Nanoparticle Formation by ReaxFF Molecular Dynamics Simulations, Energy Fuels 31 (2017) 8434–8444. DOI: 10.1021/acs.energyfuels.7b01194.

[15] C. Chen and X. Jiang, Molecular dynamics simulation of soot formation during diesel combustion with oxygenated fuel addition, Phys. Chem. Chem. Phys. 22 (2020) 20829–20836. DOI: 10.1039/D0CP01917H.

[16] A. C. T. van Duin, S. Dasgupta, F. Lorant, and W. A. Goddard, ReaxFF: A Reactive Force Field for Hydrocarbons, J. Phys. Chem. A 105 (2001) 9396–9409. DOI: 10.1021/jp004368u.

[17] C. Ashraf and A. C. T. van Duin, Extension of the ReaxFF Combustion Force Field toward Syngas Combustion and Initial Oxidation Kinetics, J. Phys. Chem. A 121 (2017) 1051–1068. DOI: 10.1021/acs.jpca.6b12429, eprint: 28072539.

[18] K. Chenoweth, A. C. T. van Duin, and W. A. Goddard, ReaxFF Reactive Force Field for Molecular Dynamics Simulations of Hydrocarbon Oxidation, J. Phys. Chem. A 112 (2008) 1040–1053. DOI: 10.1021/jp709896w.

[19] A. P. Thompson, H. M. Aktulga, R. Berger, D. S. Bolintineanu, W. M. Brown, P. S. Crozier, P. J. In 't Veld, A. Kohlmeyer, S. G. Moore, T. D. Nguyen, R. Shan, M. J. Stevens, J. Tranchida, C. Trott, and S. J. Plimpton, LAMMPS - a flexible simulation tool for particle-based materials modeling at the atomic, meso, and continuum scales, Comput. Phys. Commun. 271 (2022) 108171. DOI: 10.1016/j.cpc.2021.108171.

[20] F. Castro-Marcano, A. M. Kamat, M. F. Russo, A. C. T. van Duin, and J. P. Mathews, Combustion of an Illinois No. 6 coal char simulated using an atomistic char representation and the ReaxFF reactive force field, Combust. Flame 159 (2012) 1272–1285. DOI: 10.1016/j.combustflame.2011.10.022.

[21] W. C. Swope, H. C. Andersen, P. H. Berens, and K. R. Wilson, A computer simulation method for the calculation of equilibrium constants for the formation of physical clusters of molecules: Application to small water clusters, J. Chem. Phys. 76 (1982) 637–649. DOI: 10.1063/1.442716.

[22] D. J. Evans and B. L. Holian, The Nose–Hoover thermostat, J. Chem. Phys. 83 (1985) 4069–4074. DOI: 10.1063/1.449071.

[23] M. F. Sanner, A. J. Olson, and J.-C. Spehner, Reduced surface: An efficient way to compute molecular surfaces, Biopolymers 38 (1996) 305–320. DOI: 10.1002/(SICI)1097-0282(199603)38:3<305::AID-BIP4>3.0.CO;2-Y.

[24] K. M. Mukut, S. Roy, and E. Goudeli, Molecular arrangement and fringe identification and analysis from molecular dynamics (MAFIA-MD): A tool for analyzing the molecular structures formed during reactive molecular dynamics simulation of hydrocarbons, Comput. Phys. Commun. 276 (2022) 108325. DOI: 10.1016/j.cpc.2022.108325.

[25] A. Stukowski, Visualization and analysis of atomistic simulation data with OVITO–the Open Visualization Tool, Model. Simul. Mater. Sci. Eng. 18 (2009) 015012. DOI: 10.1088/0965-0393/18/1/015012.

[26] S. Lloyd, Least squares quantization in PCM, IEEE Trans. Inf. Theory 28 (1982) 129–137. DOI: 10.1109/TIT.1982.1056489.

[27] L. van der Maaten and G. Hinton, Visualizing Data using t-SNE, Journal of Machine Learning Research 9 (2008) 2579–2605, URL: https://www.jmlr.org/papers/v9/vandermaaten08a.html.

[28] M. G. Kendall, A NEW MEASURE OF RANK CORRELATION, Biometrika 30 (1938) 81–93. DOI: 10.1093/biomet/30.1-2.81.

[29] C. Zhang, C. Zhang, Y. Ma, and X. Xue, Imaging the C black formation by acetylene pyrolysis with molecular reactive force field simulations, Phys. Chem. Chem. Phys. 17 (2015) 11469–11480. DOI: 10.1039/C5CP00926J.

[30] A. Sharma, K. M. Mukut, S. P. Roy, and E. Goudeli, The coalescence of incipient soot clusters, Carbon 180 (2021) 215–225. DOI: 10.1016/j.carbon.2021.04.065.